International Journal of Earth Sciences Knowledge and Applications
journal homepage: http://www.ijeska.com/index.php/ijeska

Research Article

e-ISSN: 2687-5993

Experimental Study of Rainfall-Runoff Process Through Calibrated Simulator; A Case Study of Auchi Polytechnic, Auchi, Edo State, Nigeria

Yahya Olotu[1,2]*, Olawale O. Olanrewaju[2], Afolabi A. Rodiya[2,3], Adesoji P. Adekunle[4]

[1]*Department of Agricultural & Bio-Environmental Engineering, Auchi Polytechnic, Auchi, Nigeria*
[2]*Department of Agricultural & Environmental Engineering, Federal University of Technology, Akure, Nigeria*
[3]*Department of Agricultural & Bio-Environmental Engineering, The Federal Polytechnic, Ado, Ado-Ekiti, Nigeria*
[4]*Lagos State Public Work Corporation, Nigeria*

INFORMATION

Article history
Received 15 January 2022
Revised 19 June 2022
Accepted 20 June 2022

Keywords
Rainfall simulator
Rainfall-runoff
Surface runoff intensities
Runoff plot
Hydrological process

Contact
*Yahya Olotu
realyahaya@yahoo.com

ABSTRACT

The relationship between rainfall-runoff is a complex hydrological process that requires technical-based approaches to investigate and understand the interaction of the hydrological variables. A calibrated rainfall simulator was developed to produce storms at seven (7) predetermined rainfall intensities (RIs) over two (2) runoff plots (RPs). The runoff plot (RP) is 0.72 m^2 and RPB is 0.5 m^2 was inserted 0.3 m into the bare sandy loam. The results of the experimentation showed the first rainfall simulation attempt (RSA) of RI of 10.8mm/hr was completely lost to infiltration from the two runoff catchment plots. Subsequently, the RSA generated surface runoff intensities (SRI) and RPB produced higher SRI and volume compared to catchment plots (RPA). Conversely, the relationship of rainfall-runoff showed co-linearity between the simulated rainfall (SR) and generated surface flow RPA and RPB with the determinant of coefficients of 0.9926 and 0.9942 at $P < 0.05$. Therefore, the study's finding is useful to develop a rainfall-runoff model under different runoff catchment areas for developing integrated water management schemes, hydraulic structures, and irrigation scheduling.

1. Introduction

Rainfall and runoff are important components of the hydrological cycle. The relationship between these components is very important for the integrated water management system, soil erosion control, and irrigation scheduling. Modeling rainfall-runoff also plays an important role in the management and planning of water resources (French et al., 1992; Karunanithi et al., 1994).

This relationship depends on some factors such as characteristics of rainfall, runoff, temperature, and infiltration (Singh and Purty, 2016). Runoff is generated when all the processes such as infiltration evaporation demands have been satisfied. The rate and volume of generated runoff (GR) depend on rainfall characteristics (rainfall intensity, rainfall duration, and rainfall variability), catchment (catchment area, shape, slope, and orientation), the soil types (mineral and organic) and nature.

Rainfall intensity is significant in generating surface and sediment yield. Raindrop impact energy is related to the surface runoff and rainfall intensity. Therefore, a high-intensity storm could be attributed to large soil detachments and transportation (Dijk, 2020). Mohamad and Ataollah (2015) indicated that the rate of surface flow and sediment transport depends on rainfall intensity (Rose, 1993).

Truman et al. (2011) compared the impact variable and constant rainfall intensity on runoff and showed that large surface runoff was generated with variable rainfall intensity at the initial stage of rainfall-runoff simulation, while more surface flow was generated at the final stage of the constant rainfall-intensity event.

Several studies have indicated that rainfall drop size distribution is directly related to the intensity. Hence, it is essential for researchers and hydrologists attempting to

produce storms of various intensities to calibrate their rainfall simulator to generate very close storms similar to the targeted rainfall. Conversely, storm intensity is one of the important design factors and considerations when designing a rainfall simulator. The kinetic energy of a raindrop determines the surface flow and soil erosion. Physical properties of SR such as fall velocity, drop size distribution, raindrop size distribution, and kinetic energy (KE) (Eigel and Moore, 1983). The K.E under natural rainfall can be computed using Equation 1.

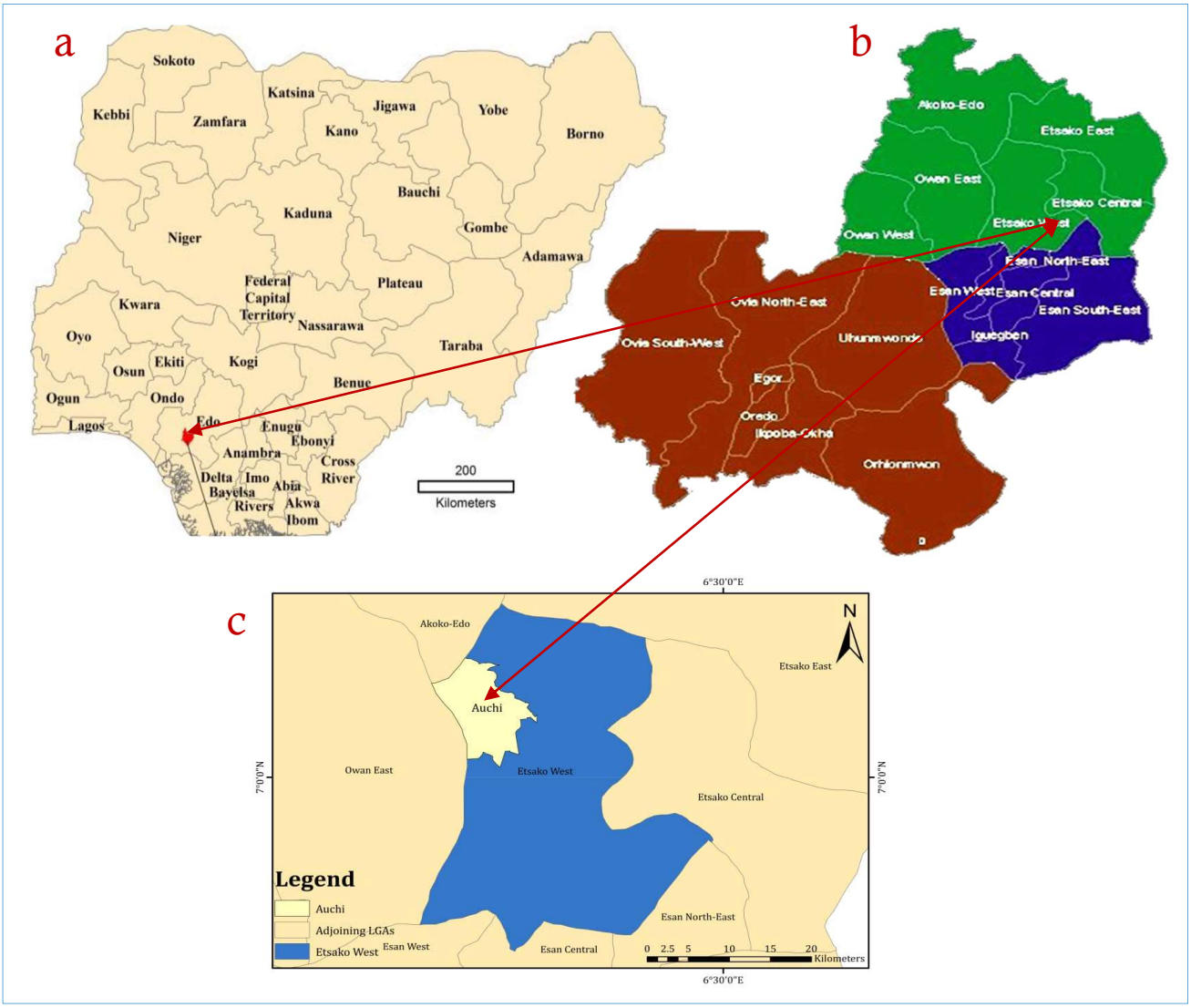

Fig. 1. a) Map of Nigeria showing Edo State, b) map of Edo North district and c) map of Auchi indicating the experimental field at Auchi Polytechnic-Campus One (Source: Author's Arcmap 10.1 Production, 2022)

$$KE = 916 + 331 log I_{10} \quad (1)$$

where; KE is Kinetic energy (ft-tons/acre-in) and I is Rainfall intensity, (in./hr)

Equation 2 can be used to calculate KE under SR for each one-minute event as follows:

$$KE_{time} = \frac{\pi}{12}\frac{1}{10^6}\frac{3600}{t}\frac{1}{A}\sum_{I=1}^{22} n_i D^3 (V_{Di})2 \quad (2)$$

where; A is the sampling area of the laser precipitation monitor (LPM), T is rainfall duration (60 s), n_i is the number of drops in the class of individual diameter range, D_i is drop class diameter (mm) and V_{Di} is the fall velocity of drops (m/s) of the diameter D_i (mm).

The average raindrop and kinetic energy can be estimated from Equations 3 and 4 as follows:

$$D_r = \sqrt[3]{\left(\frac{6}{\pi}\right)\mu} \quad (3)$$

where; D_r is raindrop diameter, (mm) and μ is average pellet weight, (mg)

Hence, KE is computed as follows:

$$KE = 0.5MV^2 \quad (4)$$

where; *KE* is kinetic energy (J), *M* is raindrop average mass (kg) and V is raindrop velocity (m/s)

Several researchers have developed and applied numerous rainfall simulators with different objectives. Kentucky rainfall simulator using design considerations such as RIs, raindrop velocities, and uniform distribution to produce similar natural rainfall conditions (Moore et al., 1983).

Estimation of a precise surface flow is useful for flood design and also important in optimum usage of precipitation in dryland farming land preparations (Vahabi and Ghafouri, 2009). Models as physically-based and conceptual have been used to simulate the rainfall processes. However, due to its complexity and Spatio variation, few models can accurately simulate this highly non-linear process (Kurien and George, 1998).

Rain simulators (RSs) are mostly used to create artificial rainfall of different intensities to study interactions among rainfall, surface runoff, and sediment yield. RSs found their application in field measurements and laboratory experiments, where the impact of weather conditions is undesirable (Stomph et al., 2002). They have been used to accelerate research on soil erosion and runoff from agricultural land and highways (Mech, 2011).

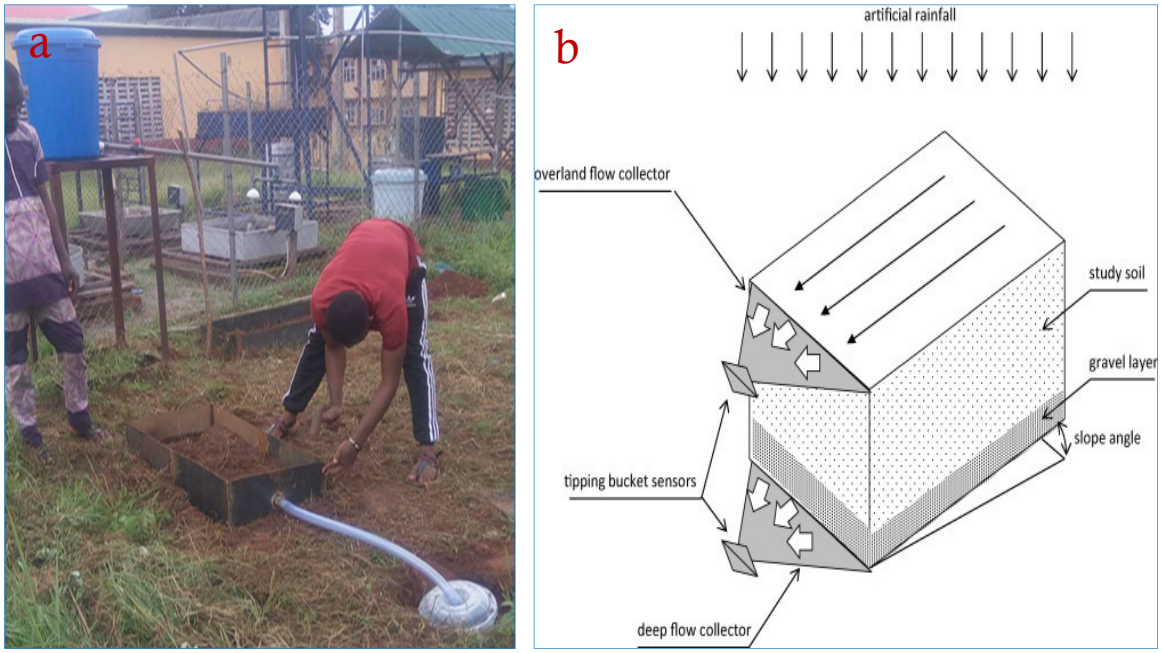

Fig. 2. a) Rainfall simulation experimental setup and b) simulator tank model (Essig et al., 2009)

This system may not reproduce rainfall accurately because the rainfall intensity is constant and raindrop kinetic energy is mostly impacted on a particular point on the soil surface. However, the laboratory experiment has its downsides, but it is very important in the simulation of surface runoff events (Micheala et al., 2017).

The effectiveness of anionic polyacrylamide to control erosion was conducted using a developed laboratory scale rainfall simulator Shoemaker et al. (2011). The simulator uses a pressure regulator and is installed at a height of 3.05 m. A high transportable and easy-operated rainfall simulator that maintains distribution, intensity, and energy characteristics of natural precipitation produced realistic output Humphry et al. (2002).

The instrument produced a storm with about 87% similarities to *KE*, a raindrop size of 1.8 mm and 70 mm/hr. rainfall intensity to the natural rainfall Chousksey et al. (2017). A precision rainfall simulator that generated an average mean drop size of 1.5 mm and energy flux was 76% similar to the expected natural rainfall intensity was developed by Abudi et al. (2012). Hence, Chousksey et al. (2017) reported that time-consuming and design complexity is the major rainfall simulator constraints. Several researchers have developed sophisticated and high-tech simulators using rotating boom, full jet cone nozzle, and vee jet noise to provide a wide range of variable and continuous intensities (Moore et al., 1983; Foster et al., 2017; Shelton et al., 2018).

The main objective of this study was to have a better understanding and knowledge of underlying surface flow generation and sediment yield in response to SR under flat and bare silty soil from two different RPs.

The result is expected to be used for the hindcast modeling and calibration of the hydrological model. In this study, a locally developed rainfall simulator to create variable RIs operated on experimental RPs of areas 0.72 m^2 and 0.5 m^2. The time response of RIs to the generation of surface runoff was computed. However, the raindrop and *KE* were computed relative to the natural rainfall.

2. Materials and methods

2.1. Study Area

The field experimentation was located in the Campus One of Auchi Polytechnic, Auchi, Edo State at latitude 7.07 N, longitude 6.26 E, and 188 m above sea level. The experimental area received an average annual rainfall of about 1211 mm and a mean temperature of 29.5 °C. The wet season ranges from April to October and 60%-80% of the annual precipitation occurs within this period. Precisely, in July and September, most of the rainfall is converted to surface and subsurface runoff due to the peak rainfall depths (RDs) during these months. The location of the study area is shown in Fig. 1.

2.2. Development of rainfall simulator and experimental setup

The simulator was developed to reproduce a storm close to natural rainfall properties such as average velocity, drop size, intensity, kinetic energy, uniformity, and distribution. The developed simulator was installed over two RPs (A and B), the RA (A) is 0.72 m^2, and the RA (B) is 0.50 m^2. The instrument contains a water supply system of 100 liters' capacity. A full jet-0.25HC30 nozzle system was used for sprinkling operation. Three nozzles were attached on 0.27cm diameter and 1meter length pipe at 0.3 m spacing designed to separate each of the nozzles from each other.

A rainfall simulator made of a 2 mm metal sheet with 0.6 m * 0.4 m dimension and adjustable feet with a minimum height of 1.3 m is used for the experiment. The simulator tank framework was constructed of angular steel supported at the four edges. Elbow joints of different diameters were used to join the PVC pipe as shown in Fig. 2a. The determination and selection of the nozzle and its spacing were based on a comprehensive review of past and current rainfall simulation studies. The experimental setup and simulator tank model are shown in Fig. 2a and Fig. 2b.

Table 1. Generated water balance parameters from RA (A) (0.72 m^2)

SR (mm)	GR (mm)	IMC (%)	FMC (%)	WC (%)	INFT (mm)
20.0	0.0	15.3	33.2	17.9	20.0
40.0	10.2	14.5	35.9	21.4	30.0
60.0	25.1	10.3	44.2	33.9	35.0
80.0	36.1	12.3	48.9	36.6	43.9
100.0	45.1	10.8	53.1	42.3	54.9
120.0	54.3	9.6	61.8	52.2	65.7
140.0	63.4	7.9	69.9	62.0	76.6

SR: Simulated rainfall; GR: Generated runoff; IMC: Initial moisture content; FMC: Final moisture content; WC: Water content; INFT: Infiltration

Table 2. Generated water balance parameters from RA (B) (0.50 m^2)

SR (mm)	GR (mm)	IMC (%)	FMC (%)	WC (%)	INFT (mm)
20.0	0.0	17.3	37.9	20.6	20.0
40.0	20.0	14.5	39.1	24.6	20.0
60.0	41.7	9.1	44.2	35.1	18.3
80.0	61.7	12.3	48.2	35.9	18.3
100.0	77.1	14.6	53.1	38.5	22.9
120.0	92.5	13.5	65.0	51.5	27.5
140.0	107.9	11.0	70.1	59.1	32.1

SR: Simulated rainfall; GR: Generated runoff; IMC: Initial moisture content; FMC: Final moisture content; WC: Water content; INFT: Infiltration

Table 3. Observed and water balance parameters from plots A and B

RI (mm/hr)	RO_A (mm/h)	RO_B (mm/h)	MSR (mm)	MRO_A (mm)	MRO_B (mm)	K_A	K_B
10.8	0.0	0.0	28.3	1.5	3.5	0.0	0.0
12.6	10.2	20.0	45.0	12.0	21.9	0.3	0.5
14.4	25.1	41.7	61.7	22.6	40.3	0.4	0.7
15.0	36.1	61.7	78.3	33.1	58.7	0.5	0.8
15.2	45.1	77.1	95.0	43.7	77.1	0.5	0.8
15.2	54.3	92.5	111.7	54.3	95.5	0.5	0.8
15.3	63.4	107.9	128.3	64.8	113.9	0.5	0.8

RI: Rainfall intensity; RO_A: Surface runoff from plots A; RO_B: Surface runoff from plots B; MSR: Modelled rainfall; MRO_A: Simulated runoff from plot A; MRO_B: Simulated runoff from plot B; K_A: Runoff coefficient for plot A; K_B: Runoff coefficient for plot B

2.2.1. Calibration of rainfall simulator

A number of 15 catch cans of 0.1 m in diameter was placed at spacing (25 cm * 25 cm) to collect water under varying pressure of 0.5 kg/cm^3, 1.0 kg/cm^3, 1.5 kg/cm^3 and 2.0 kg/cm^3 respectively. The volume of collected rainwater was converted to the millimeter using Equation 5.

However, Equation 6 was used to estimate SR uniformity.

$$R_d = \frac{V(cm^3)}{A(cm^2)} \quad (5)$$

where; Rd is Rainfall depth (cm), V is Collected rainfall volume (cm^3) and A is Orifice area (cm^2).

Rd is converted to the nearest (mm) by the value of 1000 (Olotu et al., 2014).

$$CU = 100\left(1 - \left[\frac{\sum_{i=1}^{i=n} X_i - X}{X}\right]\right) \quad (6)$$

where; CU is the mean rainfall intensity (mm h^{-1}), n is the number of observations and X_i (i = 1, 2. …..n) are the individual observations.

2.2.2. RPs design and installation

The RPs were constructed from 2mm mild steel to prevent blending. The plot (A) is 1.2 m x 0.6 m, while (B) is 1.0 m x 0.5 m, a height of 0.25m each. Each of the RPs was driven into the bare soil at an angle of 5° and to the depth of 0.125 m as depicted in Fig. 1. The RIs of 10.8 mm/hr, 12.6 mm/hr, 14.4 mm/hr, 15.0 mm/hr, 15.2 mm/hr., and 15.3 mm/hr were simulated on the runoff experimental plots. The generated surface runoff volume from the simulation attempts was converted to the depth in millimeters in Equations 7 and 8.

$$R_{oda} = \frac{RV_{a(m^3)}}{A_a(m^2)} \quad (7)$$

$$R_{odb} = \frac{RV_{b(m^3)}}{A_b(m^2)} \quad (8)$$

where; R_{oda} is runoff depth (mm) from plot (A), R_{odb} is the runoff depth from plot (B), RV_a is runoff volume from plot A and RV_b is runoff volume from plot B.

A_a and A_b are the runoff catchment areas for plots A and B (Olotu et al., 2014).

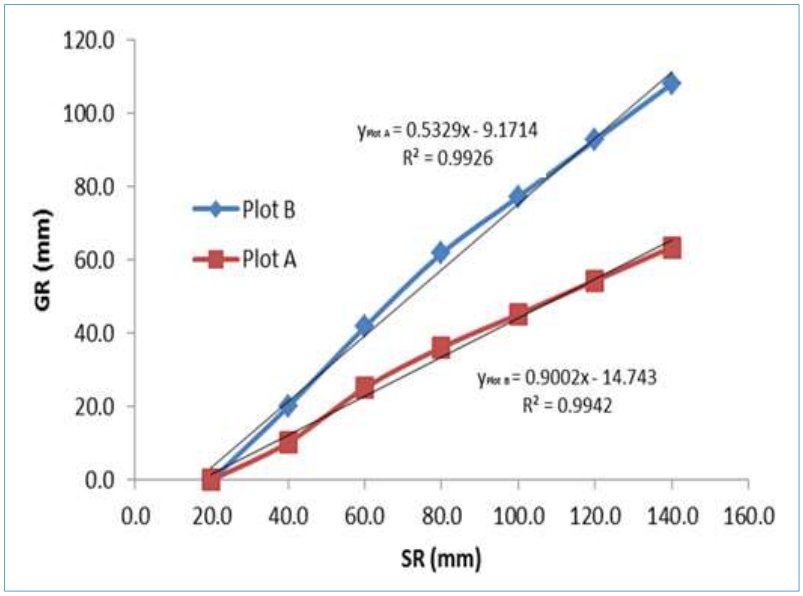

Fig. 3. Relationship between SR and GR over the RPs

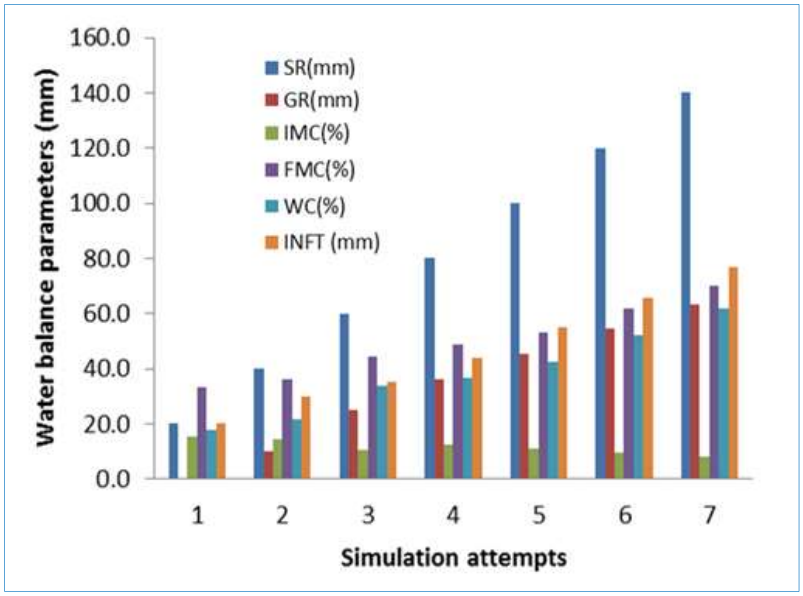

Fig. 4. Number of simulations

Table 4. Model summary for RO_A

Model 1	R	R^2	Adjusted R^2	Standard error of the estimate	Change statistics					Durbin-Watson
					R^2 Change	F Change	df1	df2	Sig. F Change	
1	0.996[a]	0.993	0.991	2.17098	0.993	674.728	1	5	0.000	0.087

a. Predictors: (Constant), SR (mm)
b. Dependent Variable: RO_A (mm)

Table 5. Model summary for RO_B

Model 1	R	R^2	Adjusted R^2	Standard error of the estimate	Change statistics					Durbin-Watson
					R^2 Change	F Change	df1	df2	Sig. F Change	
1	0.997[a]	0.994	0.993	3.25988	0.994	854.031	1	5	0.000	0.790

a. Predictors: (Constant), SR (mm)
c. Dependent Variable: RO_B (mm)

2.3. Estimation of raindrop size

The application of SR is important in the study of erosion and infiltration based on the assumption that SR produces storm events very close to natural rainfall. However, raindrop size ranges from 6-7mm in diameter and storm intensity determines the median diameter (Hudson, 1993). Raindrop size was determined using the flour pellet method as described by Hudson (1993). A tray of size 0.05 m^2 flour was exposed to a SR event for a period of 1s and 2s, respectively. The flour was oven dried for 24 hours at ambient temperature between 28-30 °C, and pellets formed were passed through an array of sieves (4.75, 3.35, 1.18, and 0.85). The pellets were measured and weighed after it was subjected to drying for 24 hours at 105 °C. To prevent the splash effects, the test area was restricted to the center of the collection tray and a test duration of 1-2s was strictly adhered to prevent duplication of count drops.

3. Results and Discussion

3.1. Generation of hydrological variables

The results in Tables 1 and 2 showed the generation of hydrological variables as surface runoff (GR), initial moisture content (IMC), and others when subjected to various SR attempts under RPs (A and B). The relationship between the SR and generated GR indicated that large surface flow was observed at plot B (0.5 m^2) under each rainfall simulation attempt, whereas more infiltration was recorded in plot A (0.72 m^2).

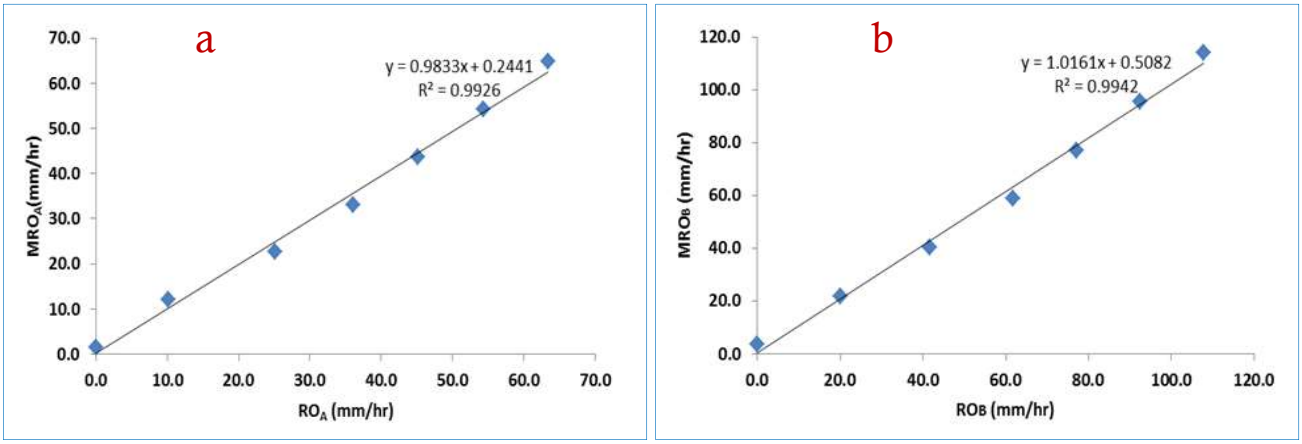

Fig. 5. a) Calibration of modeled and GR in A and b) calibration of modeled and GR in B

Based on these observations, it was deduced that surface flow was quickly generated in plot B due to its small catchment area which allowed the watershed to contribute to an initial runoff under less concentration time. Hence, the infiltration depth (INFT) is low in plot B, while INFT is high in plot A due to its large catchment area, thereby creating a more extended period for surface flow to be generated. However, the established relationship of rainfall-runoff for each catchment plot (A and B) indicated a robust relationship between the variables (SR and GR) with R^2 = 0.9942 for B and 0.9926 for plot A at P<0.05 as shown in Fig. 3.

The finding agrees with the study Singh and Purty (2016) showed that rainfall-runoff established in the East Singhblum District showed a good correlation between the hydrological variables with a coefficient of determination value of 0.99. The early initial response of runoff generation from the small RA (B) under SR is similar to the investigation of Olotu et al. (2014) showed that smaller RA $ABCD_a$ generated higher surface flow than large plot $EFGH_m$. The field experimental was investigated with seven (7) SR attempts using RDs of 20.0 mm, 40.0 mm ……140.0 mm with an incremental of 20.0 mm per simulation attempt (Tables 1, 2) (Fig. 4). The

RD corresponded to selected RIs of 10.8 mm/hr, 12.6 mm/hr, 14.4 mm/hr, 15.0 mm/hr, 15.2 mm/hr, and 15.3 mm/hr. The investigations were conducted on RPs A (1.2 m x 0.6 m) and B (1.0 m x 0.5 m) as shown in Table 3.

Table 6. Experimental and modeled rainfall index

ORI (mm/hr)	MRI (mm/hr)	OEI	MEI
10.8	10.4	443.4	424.4
12.6	12.1	517.3	493.8
14.4	13.8	591.2	563.1
15	14.4	615.8	587.6
15.2	14.6	624.1	595.7
15.3	14.7	628.1	599.8

3.2. Effects of RIs on surface runoff

During the field experimentation, seven (7) RIs were applied as precipitation events for each of the RPs A and B as shown in Table 3. The surface coefficients for plots A (K_A) and B (K_B) were estimated using Shoemaker et al. (2012) approach as the ratio of the volume of SR at each simulation attempt. Applied RI of 10.8 mm/hr generated 0.0 mm/hr for plots A and B respectively. This indicated that the SR was lost to infiltration. Conversely, the second simulation attempt of 12.6 mm/hr generated 10.2 mm/hr and 20.0 mm/hr for RO_A and RO_B (Table 3).

The experimental results showed that the size of the runoff plot is significant to the volume and intensity of generated surface runoff. The relationship between SR and surface runoff (GR) from plots A and B showed a linear trend with the $R^2 = 0.993$ and 0.994 at $P < 0.01$ in Tables 4 and 5. Hence, it was deduced that increases in surface runoff are related to increases in rainfall intensities. This observation confirms the findings from other studies where high rainfall intensity increases runoff intensity and volume (Karunanithi et al., 1994; Dijk et al., 2002; Olotu et al., 2014).

The results in Figs. 5-7 showed the established mathematical relationship between the modeled surface runoff and simulated rainfall. Conversely, a strong relationship exists between the hydrological variables with $R^2 = 0.9926$, 0.9942, and 0.9984 for the modeled surface runoff (MRO_A), generated surface runoff (RO_A), MROB and RO_B, and modeled simulated rainfall (MSR) and SR for plot A and B.

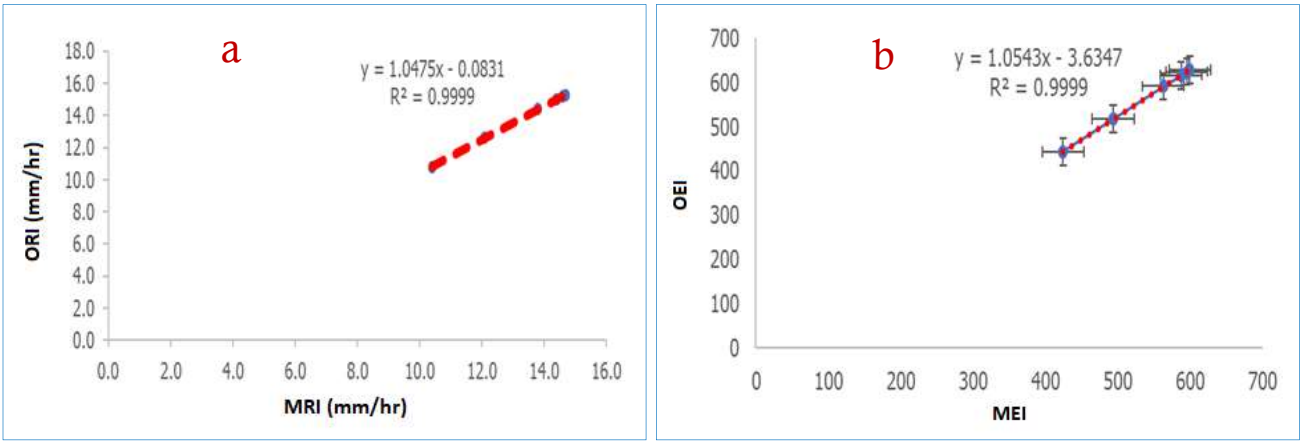

Fig. 6. a) Relationship between experimental and theoretical RIs and b) calibration of experimental and modeled EI

3.3. Rainfall index

Table 6 presents the experimental and modeled rainfall intensities (MRI) for the simulation attempts. The observed rainfall intensities (ORI) were applied to compute MRI. Hence, erosivity index (EI) was computed over the catchment plots using MRI as an input variable. Hence, EI was computed over the catchment plots using MRI as an input variable. The result shows that a higher rainfall intensity at each simulation corresponded to a large EI (Table 6 and Fig. 6a).

Hence, a determination of coefficient R^2 value of 0.999 indicated a close relationship between the experimental and modeled IRs (Fig. 2a). However, this indicates a reliable approach to estimating theoretical rainfall intensity using observed datasets (Fig. 2b). The finding shows similarity with the study of Ricks et al. (2019) which revealed that relative error between the theoretical and experimental values decreased with increases in rainfall intensities.

3.4. Drop size distribution

The experimental and modeled raindrop size diameter (RSD) produced under various RIs is presented in Table 7. The observed raindrop diameter (ODD) and MDD ranged from a minimum value of 0.61 mm; 0.90 mm at 14.4 mm/hr (ORI) and 13.8 mm/hr (MRI). However, the higher experimental and theoretical values of 1.20 mm and 1.33 mm were

produced under 15.3 mm/hr (ORI) and 14.7 mm/hr (MRI) as presented in Table 7.

The hindcast hydrological analysis of the RIs shows the possibility of generating large rainfall volume and surface flow within a short duration. Also, the result in Table 6 indicates that raindrop diameter increases with an increase in rainfall intensity and raindrop mass. The regression analysis of the relationship between the raindrop diameter size and mass showed linear expression with R^2 values of 0.979 for ODD and raindrop mass (RDM) and 0.9306 for the MDD and RDM (Fig. 7).

Table 7. Drop size distribution

ORI (mm/hr)	MRI (mm/hr)	ODD(mm)	MDD(mm)	RDM (mg)
10.8	10.4	0.79	0.98	1.78
12.6	12.1	0.93	1.04	2.07
14.4	13.8	0.61	0.90	1.34
15.0	14.4	1.00	1.21	2.24
15.2	14.6	1.12	1.24	2.74
15.3	14.7	1.20	1.33	3.01

The finding is very related to the studies of Varikoden et al. (2010) on rainfall classification, Suhaila and Jemain (2012) based on rainfall intensity and annual rainfall, and Sanchez-Moreno et al. (2012) on the relationship between kinetic energy and rainfall intensity.

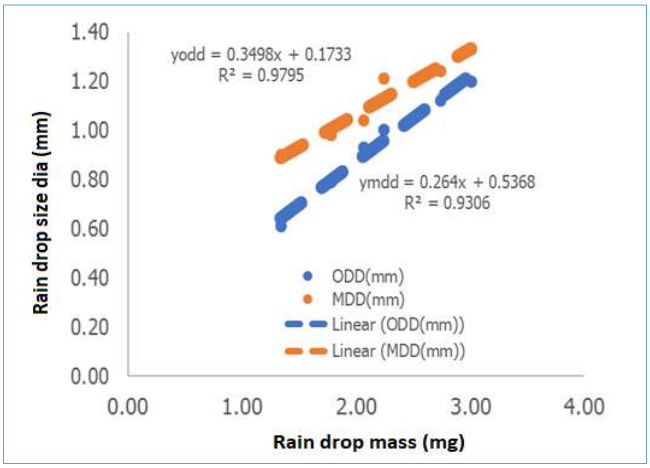

Fig. 7. Calibration of raindrop size diameter and mass

6. Conclusions

Understanding the mechanism of rainfall-runoff is significant to designing a robust integrated water management scheme and hydraulic structures for water conservation and erosion control. However, it is important to have a detailed characteristic of the rainfall-runoff relationship from the natural and artificial processes to build solid hydraulic models and similitudes. Hence, the application of a rainfall simulator is generally used to understand the surface flow, soil loss, infiltration processes, soil erodobility and EI. This study evaluated the response of various RIs (10.8 mm/hr, 12.6 mm/hr, 14.4 mm/hr, and 15.3 mm/hr) on the two bare RPs A and B on sandy loamy soil. The result of the field experiments showed that the first simulation attempt of rainfall intensity and volume of 10.8 mm/hr and 20.0 mm generated no surface runoff, the whole simulated rainfall was lost to infiltration, and the subsequent simulations generated a surface flow of varying volume, intensity, and runoff coefficient. The finding showed that the smaller runoff plot generated higher surface flow than the large catchment plot under the same rainfall intensity, simulation height (3.5 m), and slope angle of inclination (5°). The result from the study indicated the effect of rainfall intensity on RSD and EI from the experimental and theoretical simulation. Hence, it is revealed that EI and RSD were dependent on rainfall intensity. The overall study's result is very significant for developing a rainfall-runoff model capable of solving soil loss and erosion events. However, to further characterize rainfall variables, the study recommends future work to test, evaluate, and calibrate simulation height, rainfall intensity, and slope of runoff catchment plot.

References

Abudi, I., Carmi, G., Berliner, P., 2012. Rainfall simulator for field runoff studies. Journal of Hydrology 10 (2), 76-81.

Chouksey, A., Lambey, V., Nikam, B.R., Aggarwal, S.P., Dutta, S., 2017. Hydrological modelling using a rainfall simulator over an experimental hillslope plot. Hydrology 4 (1), 1-20.

Dijk, A.I.J.M., Bruijnzeel, L.A., Rosewell, C.J., 2002. Rainfall intensity-kinetic energy relationships: a critical literature appraisal. Journal of Hydrology 261 (45), 1-28.

Eigel, J.D., Moore, I.D., 1983. A Simplified Technique for Measuring Raindrop Size and Distribution. Transactions of the ASABE 26 (4), 1079-1084.

Essig, E.T., Corradini, C., Morbidelli, R., Govindaraju, R.S., 2009. Infiltration and deep flow over sloping surfaces: comparison of numerical and experimental results. Journal of Hydrology 374, 30-42.

French, M.N., Krajewski, W.F., Cuykendall, R.R., 1992. Rainfall Forecasting in Space and Time Using a Neural Network. Journal of Hydrology 137 (1-4), 1-31.

Foster, G.R., Neibling, W.H., Natterman, R.A., 2017. A Programmable Rainfall Simulator. American Society Agricultural Engineers: St. Joseph, MI, USA.

Hudson, N.W., 1993. Field Measurement of Soil Erosion and Runoff, Food and Agriculture Organization of the United Nations, Rome, Italy.

Humphry, J.B., Daniel, T.C., Edwards, R.D., Sharpley, A.N., 2002. A portable rainfall simulator for pilot scale runoff studies. Applied Engineering in Agriculture 18 (2), 199-204.

Karunanithi, N., Grenney, W.J., Whitley, D., Bovee, K., 1994. Neural Networks for River Flow Prediction. Journal of Computing in Civil Engineering 8 (29), 201-220.

Kurien, E.K., George, T.P., 1998. Design, fabrication and testing of a rainfall simulator. Proc. Tenth Kerala Science Congress. pp.

63-65.

Mech, S., 2011. Limitations of simulated rainfall as a research tool. Transactions of the ASAE 8 (1), 66-75.

Micheala, D., Peter, V., Roman, V., 2017. Evaluation of surface runoff generation processing using a rainfall simulator: A small scale laboratory experiment. IOP Conference Series Earth and Environmental Science 95 (2), 20-28.

Mohamad, A., Ataollah, K., 2015. Effects of rainfall patterns on runoff and soil erosion in field plots. International Soil and Water Conservation Research 3 (4), 273-281.

Moore, I.D., Hirschi, M.C., Barfield, B.J., 1983. Kentucky rainfall simulator. Transactions of the ASAE 26, 1085-1089.

Olotu, Y., Bada, O., Rodiya, A.A., Omotayo, F.S., 2014. Sensitivity-Based Modeling of Evaluating Surface Runoff and Sediment Load Using Digital and Analog Mechanism. Global Journal of Science Frontier Research 14 (3), 1-9.

Ricks, M.D., Matthew, A.H., Faulkner, B., Zech, W.C., Fang, X., Wesley, N.D., Perez, M.A., 2019. Design of a pressurized rainfall simulator for evaluating the performance of erosion control practices. Water 11 (2), 1-18.

Rose, C.W., 1993. Erosion and sedimentation. In: M. Bonell, M.M. Hufschmidt, J.S. Gladwell (Eds.), Hydrology and Water Management in Humid Tropics, Cambridge University Press, Cambridge.

Sanchez-Moreno, S., Matthew, A.H., Hirschi, N.K., 2012. Rainfall kinetic energy-intensity and rainfall momentum-intensity relationship for Cape Verde. Journal of Hydrology 454-455, 131-140.

Shelton, C.H., von Bernuth, R.D., Rajbhandari, S.P., 2018. A continuous-application of rainfall simulator. Transactions of the ASAE 28 (4), 1115, 1119.

Shoemaker, A.L., Zech, W.C., Clement, T.P., 2012. Laboratory-Scale Evaluation of Anionic Polyacrylamide as an Erosion and Sediment Control Measure on Steep-Sloped Construction Sites. Transaction of the ASABE 55(3), 809-815.

Singh, P.K., Purty, P., 2016. Estimation of rainfall-runoff relationship in East Singhbhum District, Jharkhand, India. BEST: International Journal of Management, Information Technology and Engineering 4 (10),15-28.

Stomph, T.J., de Ridder, N., Steenhuis, T.S., van de Giesen, N.C., 2002. Scale effects of Hortonian overland flow and rainfall-runoff dynamics: Laboratory validation of a process-based model. Earth Surface Processes and Landforms 27 (2), 847-855.

Suhaila, J., Jemain, A.A., 2012. Spatial analysis of daily rainfall intensity and concentration index in Peninsular Malaysia. Theoretical and Applied Climatology 108 (1-2), 235-245.

Truman, C.C., Potter, T.L., Nuti, R.C., Franklin, D.H., Bosch, D.D., 2011. Antecedent water content affects runoff and sediment yields from two Coastal Plain Ultisols. Agricultural Water Management 98, 1189-1196.

Vahabi, J., Ghafouri, M., 2009. Determination of Runoff Threshold Using Rainfall Simulator in the Southern Alborz Range Foothill-Iran. Research Journal of Environmental Sciences 3(1), 193-201.

Varikoden, H., Samah, A.A., Babu, C.A., 2010. Spatial and temporal characteristics of rain intensity in peninsular Malaysia using TRMM rain rate. Journal of Hydrology 387 (3-4), 312-319.